

مركز مصر للأشعة
MISR RADIOLOGY
CENTER



لأول مرة في أفريقيا
و الشرق الأوسط

PET/MRI 3-TESLA



Where and why it might replace PET/CT?

- **Better TNM staging** due to magnificent spatial resolution and great soft tissue details.
- **Same cost (or even less)** in cases where both PET/CT and MRI are indicated.
- **Significantly reduced radiation dose.**
- **Reduced tracer dose.**
- Novel MR sequences to **minimize** the susceptibility artifacts of metallic implants.

Benefits of Simultaneous Imaging

- **Shorter study time** as it integrates both PET and MRI studies in a simultaneous process.
- Simultaneous acquisition **reduces error** in combined interpretation of MR physiologic and PET metabolic data.
- **Ensuring** that MR physiologic data and PET metabolic data reflect the **same biological state**, eliminating the chance that change in therapy between separate imaging sessions may cause discordant results.
- SIGNA PET/MR scanner has TOF capability which improves signal-to-noise ratio compared to non-TOF images.



Brain Tumors

18F-DOPA PET/MR of non enhancing WHO grade III oligodendroglioma

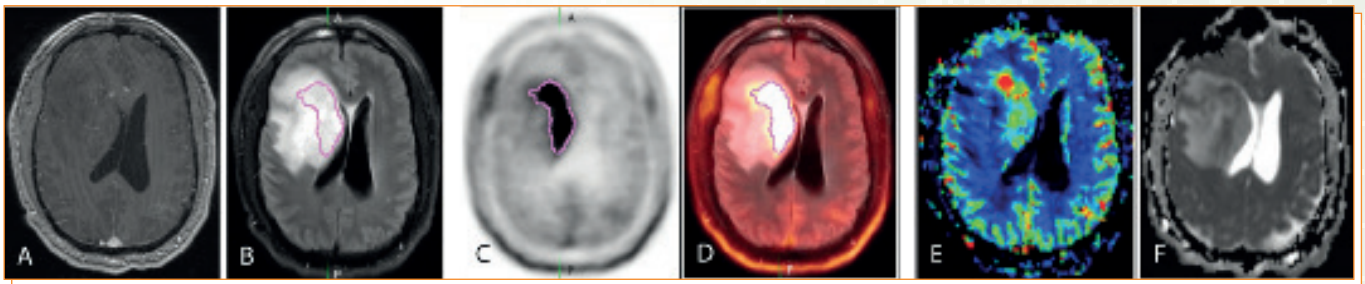
A) Axial post-contrast T1WI

B) Axial FLAIR

C) Unfused 18F-DOPA PET

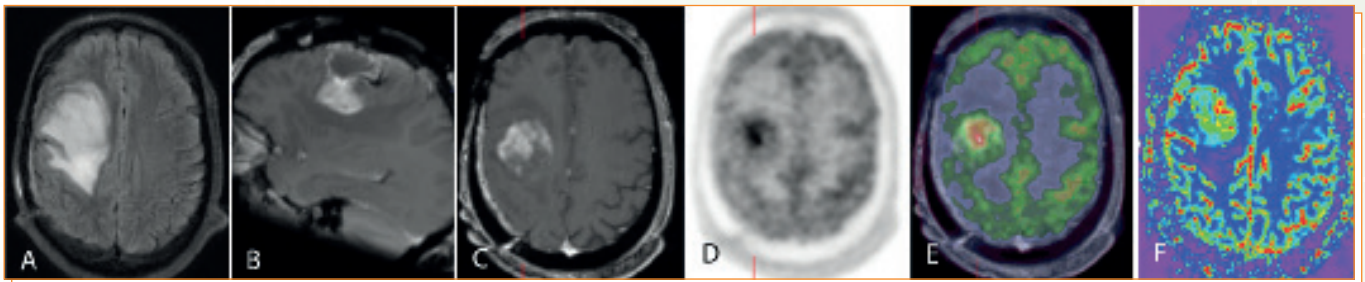
D) Fused 18F-DOPA PET to FLAIR

shows uptake in a portion of the abnormal tissue with a region of interest demarcating greatest 18F-DOPA uptake and suspected non enhancing high grade tumor. The 18F-DOPA activity corresponds well to **increased rCBV (E)** and **reduced ADC (F)** which are additional MR markers of high grade tumor.



Treatment Follow Up

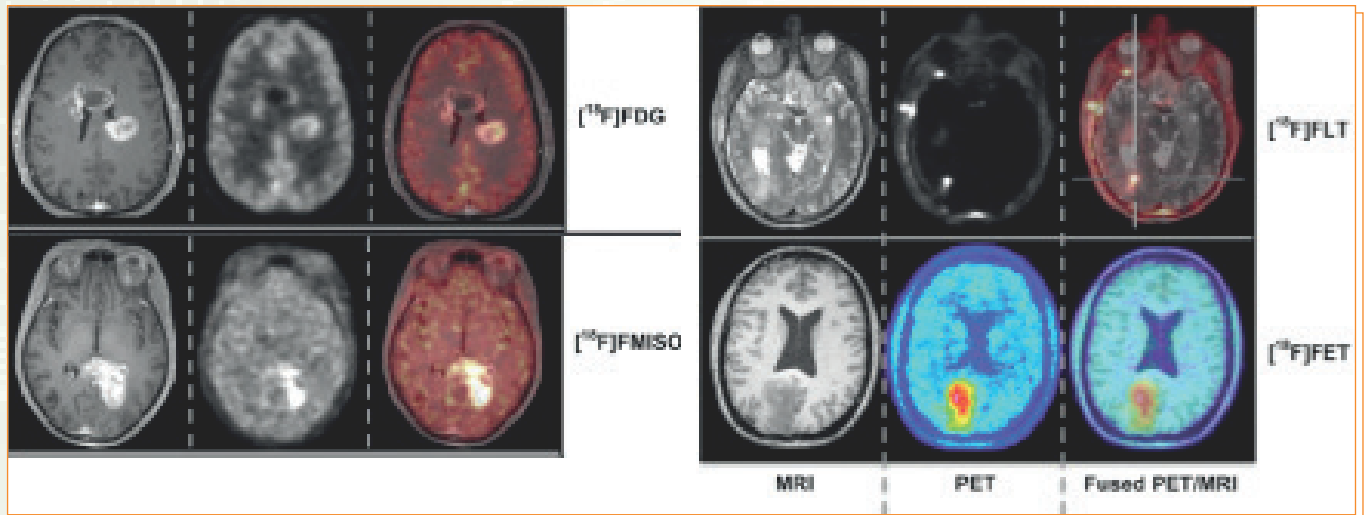
45 year old man with a history of a resected WHO grade IV GBM treated with chemotherapy and radiotherapy presents with worsening FLAIR (A) signal changes and new enhancement on contrast-enhanced T1WI (B, C) adjacent to the treatment site increased 18F-FDG uptake on unfused PET (D) and fused PET/MR (E), and elevated rCBV (F) support recurrent GBM.



Brain Tumors

Treatment Follow Up

Simultaneous PET/MR studies in patient with brain tumors (A) axial PET/MR and fused images are shown for different tracers FDG, FMISO, FLT and FET



Conclusion

Glioma Grading

Contrast enhancement, elevated rCBV, lactate peak on MRS, and low ADC suggest HGG. 18F-FDG, 11C-MET, 18F-DOPA, and 18F-MISO can differentiate HGG from LGG.

Tumor Extension

PWI, DTI/DWI, MRS, and amino acid analog PET tracers aid in determining non-enhancing tumor margins.

Treatment Follow Up

MRS, PWI, DWI, 18F-FDG PET, and amino acid PET aid in differentiating radiation necrosis and pseudo-progression from recurrent high grade glioma.

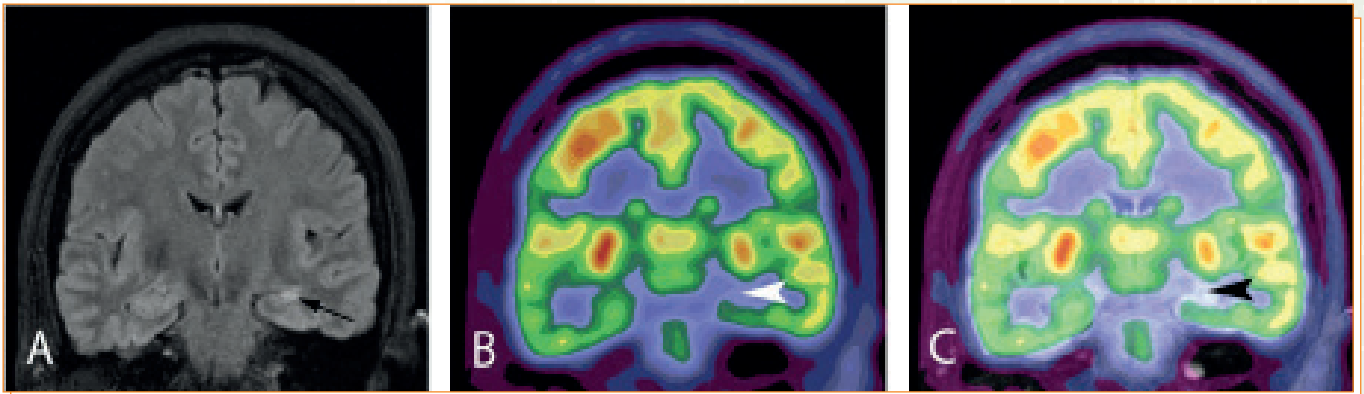
Metastatic Disease

Conventional contrast-enhanced MRI is primarily used for detection of intracranial metastatic disease and follow up after treatment.

Whole-body 18F-FDG PET/MR including dedicated contrast-enhanced brain imaging may be equivalent to PET/CT and brain MRI for staging metastatic lung cancer.

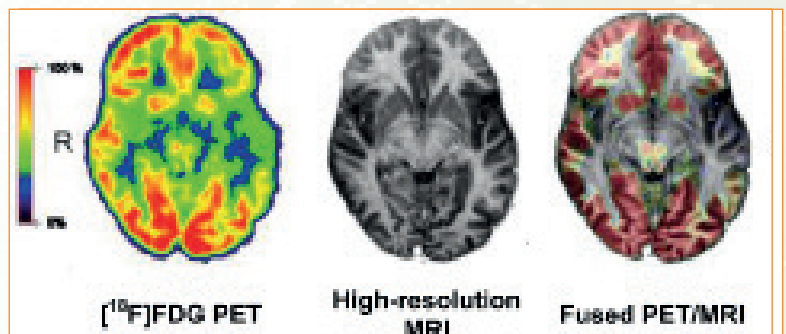
Epilepsy

PET/MR for presurgical workup of a 47 year old woman with medically refractory temporal lobe epilepsy shows classic signs of hippocampal sclerosis on the coronal FLAIR images (A) including increased signal intensity and reduced size of the hippocampus (arrow) with reduced ^{18}F -FDG uptake on the unfused PET (B) and fused PET/MR (C) (arrowhead)



Simultaneous PET/MR study in an epilepsy patient From left to right:

Axial FDG-PET (6075- min post-injection), high resolution MRI-scan and fusion image Distinct hypometabolism is visible in the polar region of the left temporal lobe, typically corresponding to the epileptogenic focus

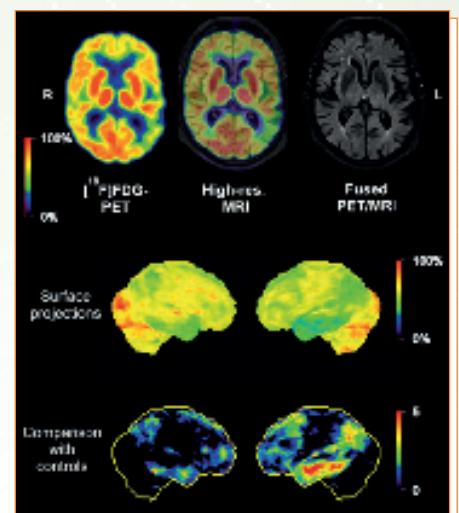


Memory Disturbances

Simultaneous PET/MR study in an AD patient

1- Upper row: axial FDG-PET, high resolution MRI and fusion image areas with reduced metabolism (green) representing impaired neuronal function are visible in the left temporo-parietal cortex

2- Lower rows: Surface projections of cerebral metabolism and of Z-scores images (comparison with controls).



Memory Disturbances

Concept

These high end state of art PET/MRI exams can be used to assess memory disturbance with aim of ruling out Alzheimer's disease (AD) or other dementias.

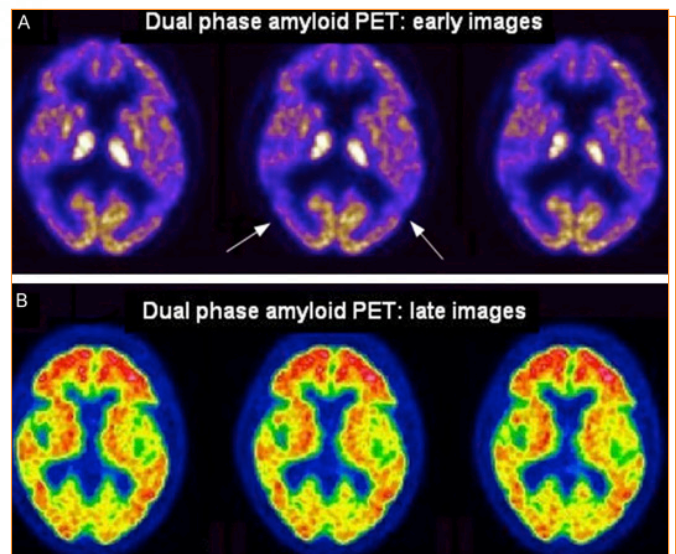
Also if proven to be early case of AD or other dementia, then rapid targeted treatment can be introduced to slow down the disease progression.

Neuroimaging of amyloid plaques

A 66-year-old female with cognitive impairment (amnesic MCI, MMSE 22/30). Patient was submitted to dual phase **amyloid PET scan with 18F-flutemetamol**.

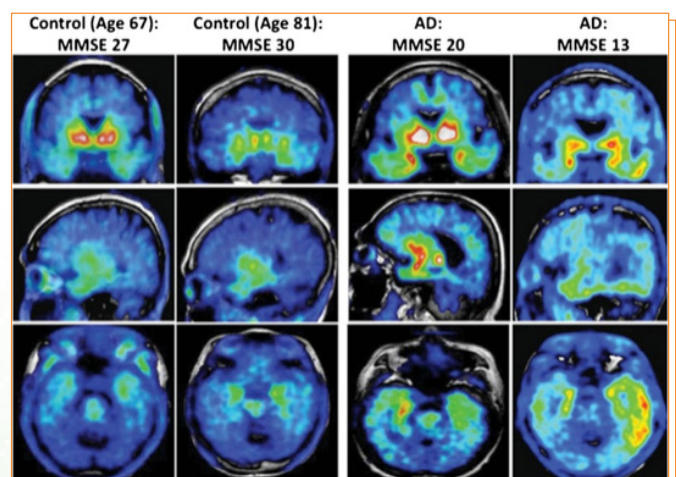
Axial early image (first row, A) showed bilateral perfusion defect in the temporo-parietal regions (white arrows) as typically found in AD patients.

Late phase (axial B) was positive for high amyloid burden. This case illustrates the potential usefulness of dual-phase amyloid imaging for the concomitant assessment of both amyloid burden and neuronal dysfunction.



PET imaging of tau protein targets

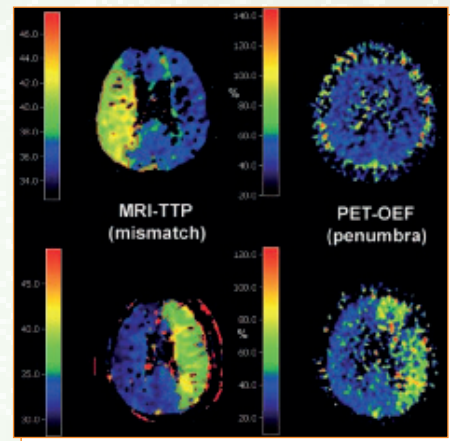
Representative **18F-THK5351** SUVR 40-60 min PET images of 4 participants (2 controls and 2 AD). These cases present different levels of binding that illustrate the dynamic range of SUVR across participants.



- Although **PET** is considered a gold standard for non-invasively identifying the relevant regions of hemodynamic and metabolic compromise in ischemic stroke, it is not routinely the first-line diagnostic evaluation of patients with suspected cerebrovascular stroke
- This is **because the PET studies** that would be the most useful in the acute phase of ischemic stroke (i.e. those **involving O-15 or C-11 labeled tracers**) are also the most challenging logistically
- So Simultaneous measurements would elucidate the ongoing debate concerning the relationship between the perfusion-diffusion mismatch and the PET penumbra (Fig.1)

Fig. 1

Comparison of MRI time-to-peak (TTP) and PET OEF images in two patients measured in the chronic phase of stroke illustrating the mismatch-penumbra debate. Disagreement between the two techniques is observed in the first (upper row) and agreement in the second case (lower row)



- **15O-H2O PET**, and subsequently **PWI**, have been used to study cerebral blood flow (**CBF**) in reversible cerebral ischemia
- **PET/MRI is the ideal imaging tool** for cerebrovascular perfusion research as it allows temporally matched correlation of DWI with quantitative 15O-H2O PET CBF
- The practical application of 15O-H2O PET to stroke research is challenging because of difficulties in supplying a radiotracer with a short half-life within the appropriate timeframe to study cerebral hemodynamics during an acute stroke

Carotid Plaque Imaging

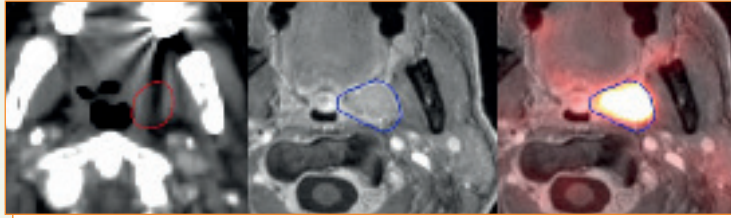
- **PET/MR** has been used for vessel wall imaging in the setting ischemic stroke of **cryptogenic origin** with complicated MR features of a carotid plaque combined with evidence of **vessel wall inflammation on 18F-FDG PET** suggesting a causal role for these plaques in the stroke
- **Conventional MR co-registered to 18F-FDG PET/CT** has been used to correct partial volume error in vessel walls, suggesting that PET/MR may add benefit to vessel wall imaging in the evaluation of plaques at risk for rupture

Head & Neck

Head & Neck

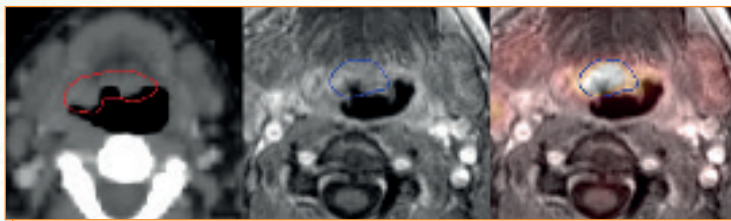
Left tonsil SCC PET/MRI showed soft tissue encroachment to the uvula not delineated on CT with a resultant increase in GTV (gross tumor volume) size

PET/MR substantially altered the primary GTV



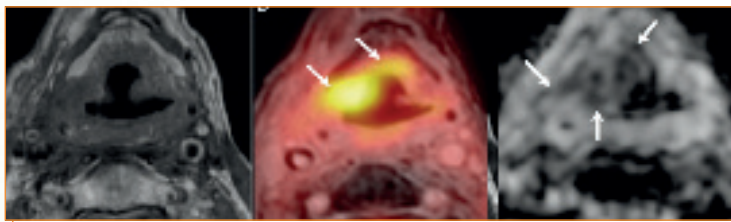
Tongue base SCC though the planning CT-GTV included indeterminate soft tissue in the right base of tongue, PET/MRI showed tumor limited to the central base of tongue with a resultant decrease in GTV size

PET/MR substantially altered the primary GTV



Positive concordant findings on MRI, DWI and PET in 69-year old male with pain 4 years after RTH/CTH for laryngeal SCC displaying Recurrent tumor within the predominant post treatment change

Local recurrence of squamous cell carcinoma of the head and neck after radio(chemo)therapy



(MTV) and (TLG) were checked as metabolo-volumetric parameters for pre-operative evaluation for 50-year patient with left tongue CC

Metabolic tumor volume (MTV) and total lesion glycolysis (TLG) as metabolo-volumetric parameters are prognostic factors for tumor aggressiveness and evaluation response to treatment



Breast

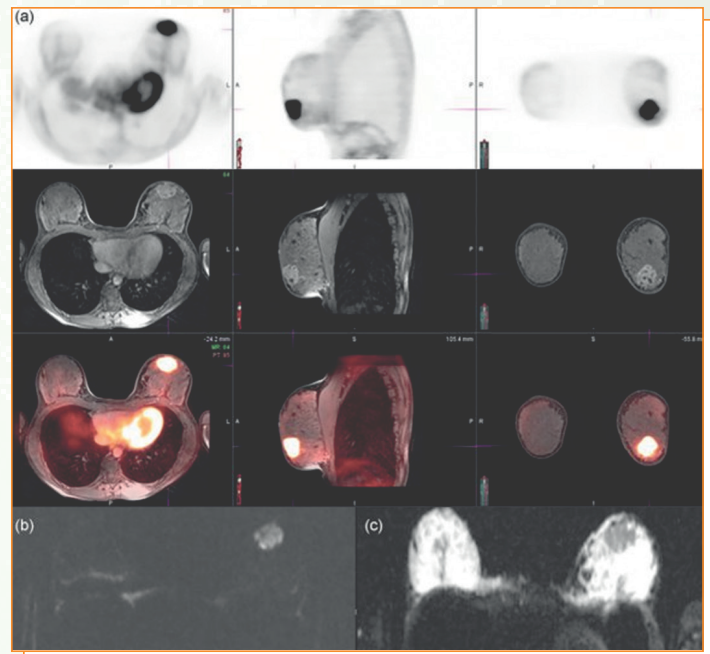
- **Breast PET/MRI** has shown promise in reducing unnecessary biopsies that would be recommended based on their current standard DCE-MRI.
- **Breast PET/MR** may be more important before and during neoadjuvant therapy, which lend increased precision to breast cancer treatments.
- In local staging, where the improved evaluation of the axilla potentially afforded by **PET/MRI** may eventually preclude the need for axillary lymph node tissue sampling.
- The inclusion of DWI in PET/MRI protocols adds sensitivity.
- In need of whole-body staging or post treatment surveillance, **PET/MR** outperforms PET/CT at a much lower radiation dose.
- To whole-body exams, PET adds specificity.

Locoregional Staging

Invasive Ductal Carcinoma

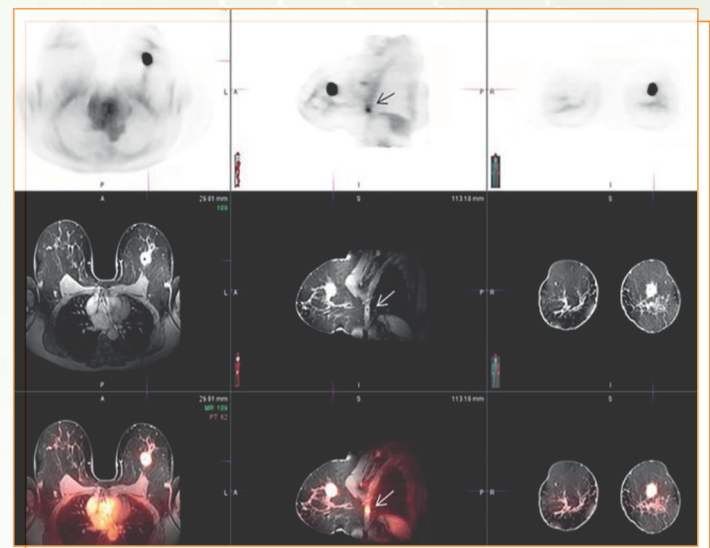
A 38-year-old female diagnosed with invasive ductal carcinoma

The index lesion is well characterized on these images as an FDG-avid heterogeneously enhancing lesion in the left breast abutting the skin surface. There was no evidence of metastatic disease at the time of the examination.



A 62-year-old female with left breast invasive ductal carcinoma and positive left axillary lymph nodes. Whole-body PET/MR detected distant metastatic disease in this patient that was not previously diagnosed

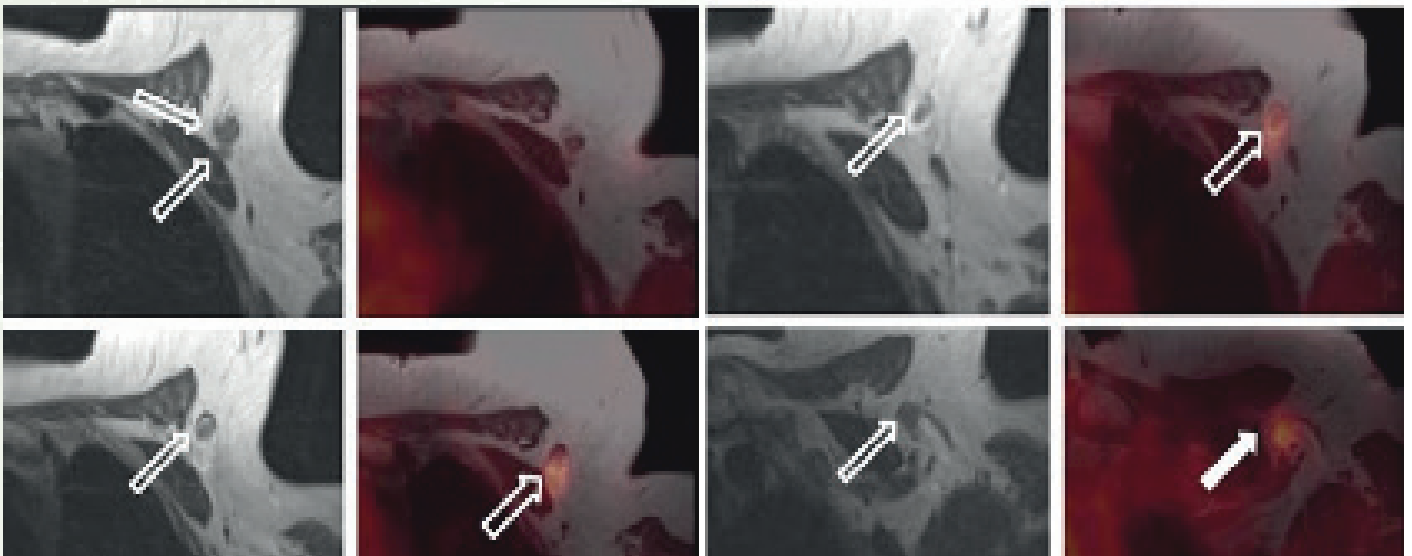
The index lesion is well characterized on these images as an FDG avidly enhancing mass in the left breast. An unexpected rib metastasis is seen enhanced on DCE MRI and is FDG-avid on PET (arrow)



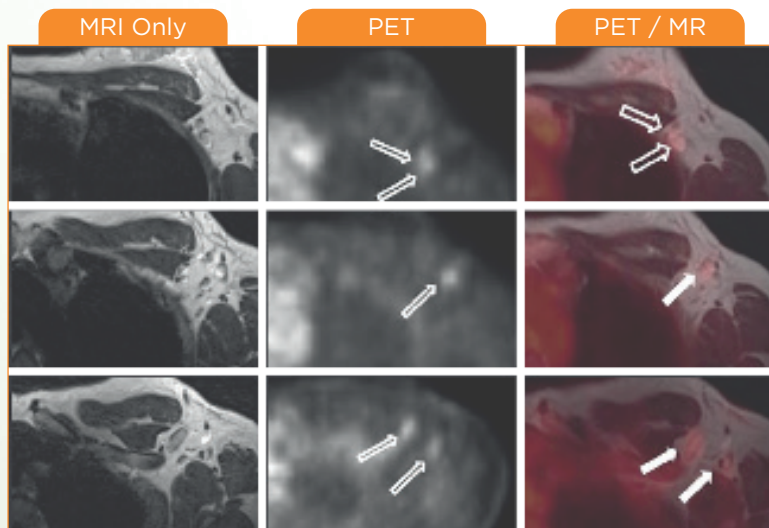
Nodal disease

LN Metastasis

- Images of a patient with three axillary lymph nodes suspicious for metastases on PET/MRI (big arrows, right column)
- Compared to five on MRI-only (small arrows left column)
- Combining PET information with MRI, resulted in three lymph nodes marked as suspicious for metastases



- Images of a patient with no lymph nodes suspicious for metastases on MRI (T2w sequence is shown in the left column)
- and five axillary FDG hotspots suspicious for lymph node metastases on PET (small arrows, middle column)
- Adding PET information to MRI, resulted in five lymph nodes marked as suspicious for metastases (big arrows, right column).



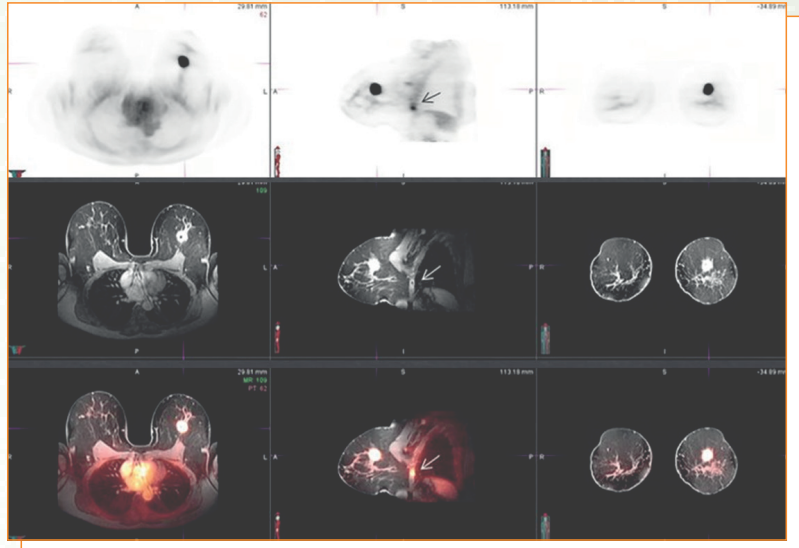
Breast

Distant Metastasis

In whole-body imaging for breast cancer, PET/MR imaging has been shown to provide improved sensitivity over PET/CT or PET alone, particularly for breast cancers, liver metastases and bone metastases. PET/MR imaging has also been shown to detect brain metastases

Rib Metastasis

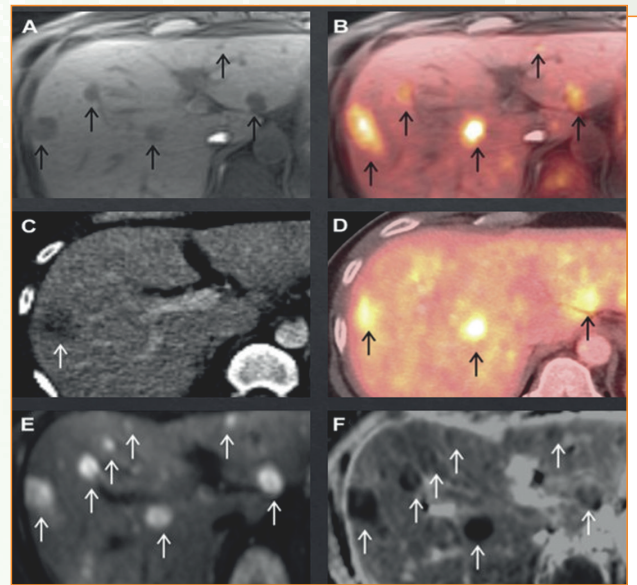
A 62-years old female, known left breast IDC with positive axillary nodes. The left breast index lesion is shown with the unexpected rib metastasis on DCE MRI and PET/MR images.



Liver Metastasis

A 56-year-old patient with a history of right breast invasive ductal cancer metastases (A) Contrast enhanced T1 weighted image demonstrates multiple liver metastases (arrows) with increased FDG uptake also readily visible on the (B) fused T1- weighted and PET image

(C) Contrast-enhanced CT image only clearly shows a single metastasis (arrow)
(D) Although the fused PET/CT image shows additional hypermetabolic lesions (arrows), high background hepatic FDG uptake makes detection more difficult than on PET/MR imaging (B)

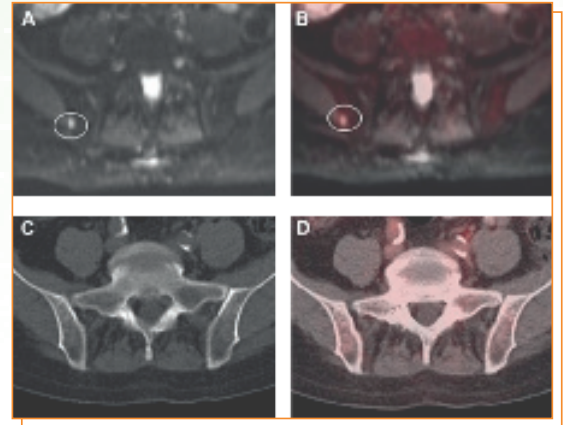


(E, F) Corresponding DWI image and ADC map from the PET/MR image demonstrate even more metastases (arrows) with restricted diffusion.

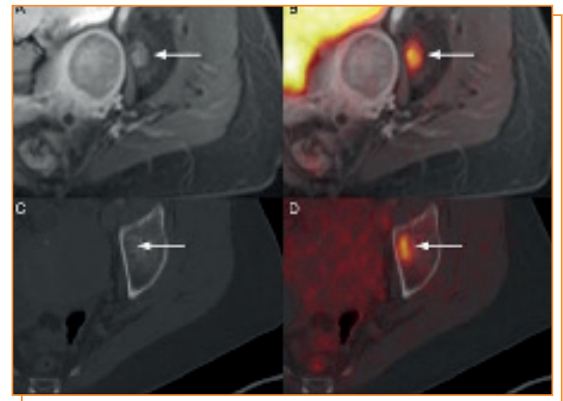
Distant Metastasis

Bone Metastasis

A 75-year-old woman, status post mastectomy for known left IDC, imaged for surveillance. (A) Diffusion-weighted imaging shows metastasis as a focus of restricted diffusion in the right ilium (circle) which demonstrates mild FDG uptake on the (B) fused T1-weighted/PET Image (circle) (C) CT and (D) fused PET/CT images show no evidence of disease at the same location



53-y-old female patient with breast cancer recurrent osseous metastasis in the left acetabulum demonstrating pathologic contrast enhancement (A) as well as focal 18-FDG uptake on PET/MRI (B) and PET/CT (D) The metastasis did not show a distinct correlate on corresponding CT images (C) and was thus missed on CT



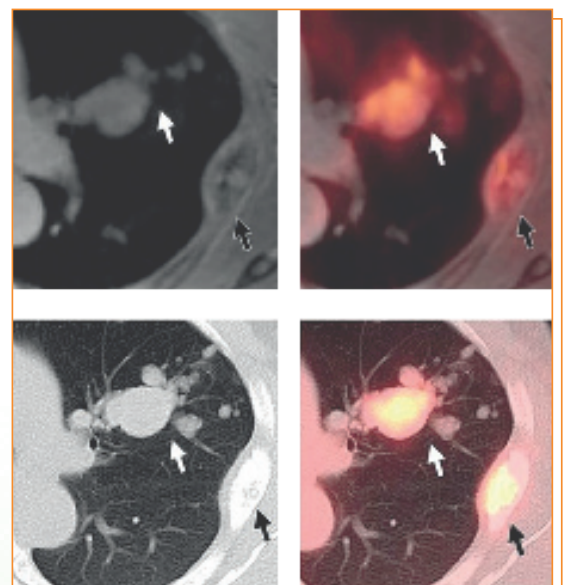
Lung & Bone Metastasis

48-y-old woman with history of left breast cancer metastatic to lung and bone obtained to monitor response during chemotherapy

a) Contrast enhanced MR and (b) PET/MR images show several lung metastasis (white arrow)

c) CT and (d) PET/CT images show these metastasis (white arrow) more clearly

An expansile rib metastasis (black arrow) is seen on all images



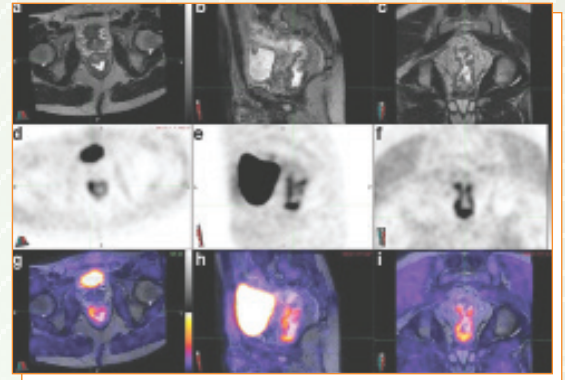
Abdomen / Retroperitoneum

Rectal

PET/MR of a patient with rectal cancer which was performed on a sequential MR/PET system. Asymmetrical thickening of the rectal wall is seen in the axial (a), sagittal (b), and coronal (c) planes of the T2 TSE sequence.

Associated increased FDG uptake in relationship to the finding described previously is seen in the PET acquisition (d-f)

Fusion images (g-i) help determine malignant origin of the thickening and the absence of involved lymph nodes

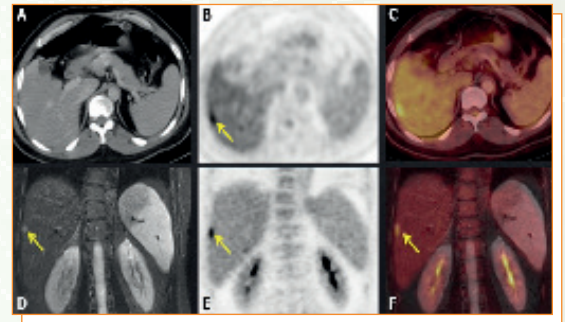


Cancer Colon

Consecutive combined abdominal PET/CT (top row) and PET/MR (bottom row) examinations of a colon cancer patient

(A) CT image does not show any lesions.

(B) a hot spot (arrow) is seen in the PET image which can be located in the liver by image fusion (C). (D) MR image shows a liver lesion (arrow) that corresponds to (E) a hot spot in a PET image and is (F) co-localized in a PET/MR fused image

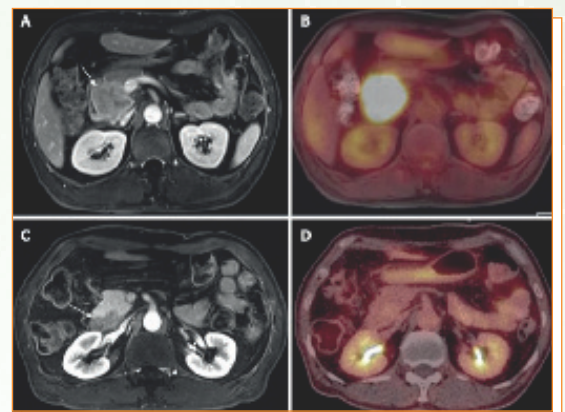


Pancreatic Cancer

A, B: A 5-cm mass of biopsy-proven adenosquamous carcinoma (arrow) in the pancreatic head, as seen due to the strong FDG uptake

C, D: The mass (arrow) shows a marked decrease in size and glucose metabolism (from 22.0 to 3.8 of mSUV) after six cycles of neoadjuvant concurrent chemoradiation treatment

The specimen obtained during surgery revealed complete remission

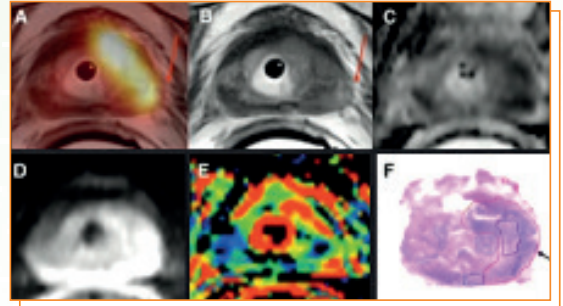


Pelvic Malignancy

Prostate

T-Staging PSMA PET-MRI

75-year-old man with PSA level of 25.6 ng/mL
A) Fused PET/MR shows left peripheral zone mass with focal increased radiotracer uptake
B) axial T2-WI shows low signal left sided-lesion
C) ADC map demonstrates restricted diffusion in left peripheral zone (arrow).

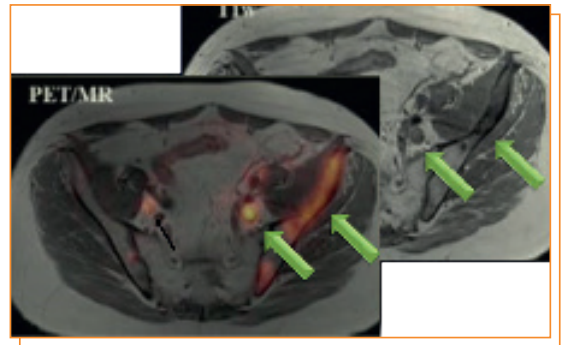


NM-Staging PSMA PET-MRI

Initial staging of a 70-year-old man with prostate cancer
Axial T1-WI (left) shows marrow infiltrative lesion of the left iliac bone as well as left sided rounded lymph node (arrows).

Fused 68Ga-PSMA PET/MR images (right) shows focal uptake (arrows) corresponding to left iliac bone and left pelvic lymph nodes on T1-weighted MRI

Note the focal uptake of tiny right pelvic lymph node (small arrow).

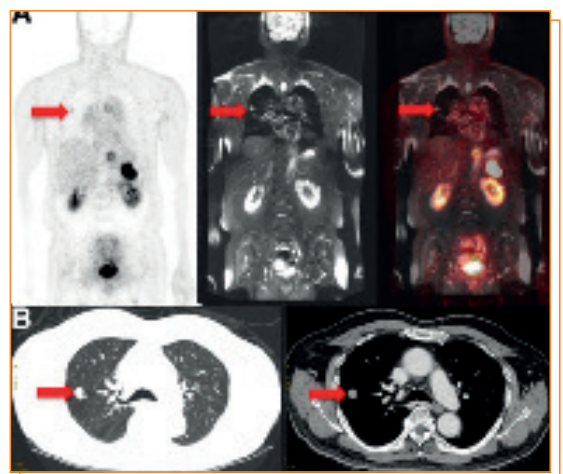


Biochemical Recurrence

A 66-year-old man with PCa treated with surgery, radiation therapy, and androgen deprivation therapy at initial presentation - Gleason score, 5+4
Now with BCR and rising PSA level (from 0.07 ng/mL initially to 10.1 ng/mL at time of scan)

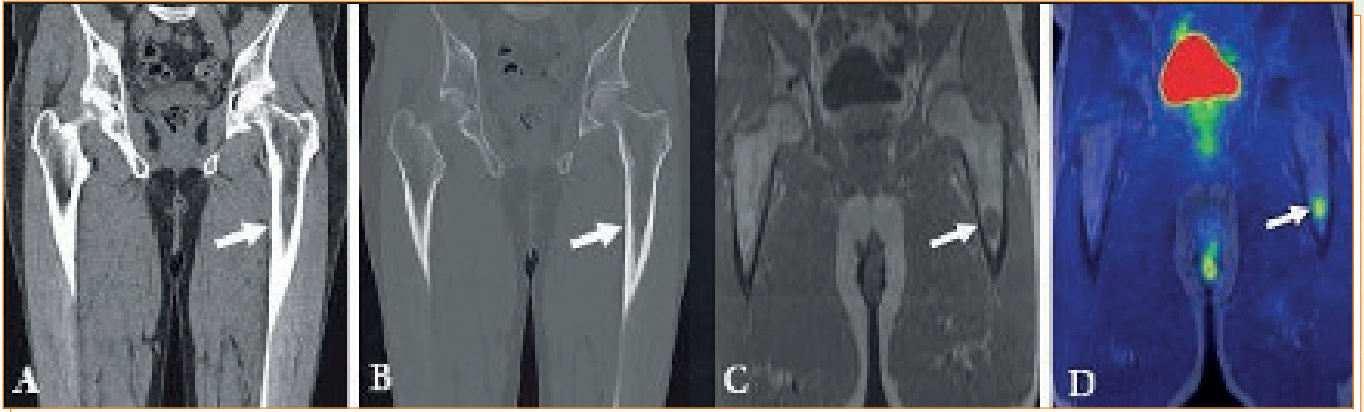
Coronal 68Ga-PSMA PET image (left) shows faint (but greater than in adjacent normal lung parenchyma) focal uptake (arrows) corresponding to lung nodule on T2-weighted MRI (middle) and fused PET/MRI right

Follow-up dedicated chest CT done 2 wk later shows lung nodule (arrows), which was biopsy-proven to represent metastatic adenocarcinoma of prostate origin



Neoplastic

Multiple Myeloma



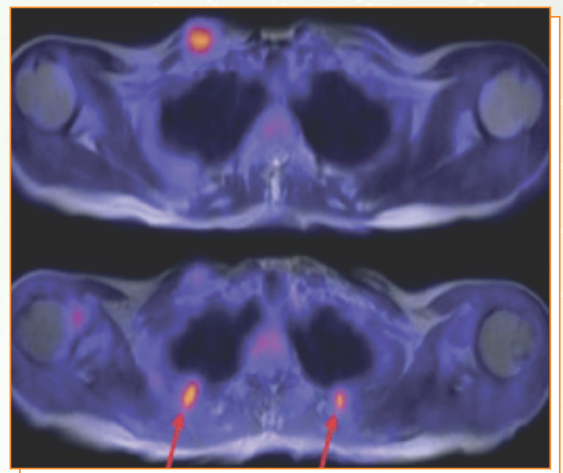
60-year-old man with history of multiple myeloma who underwent chemotherapy and had laboratory evidence of relapse restaging whole-body low-dose CT shows subtle area of soft-tissue density in proximal left femoral shaft (arrow, A) without corresponding osteolysis (arrow, B)

Subsequent FDG PET/MRI shows T1-hypointense marrow-replacing lesion in same location (arrow, C) with increased FDG activity seen on fused PET/MR image (arrow, D) consistent with active disease

CT often fails to detect early focal lesions that are not yet lytic. Owing to high soft tissue contrast and better ability to detect marrow lesions, whole body MRI has also been used for the evaluation of multiple myeloma

Pathologic Fractures

A patient previously thought to have smoldering MM presented with right clavicle fracture on light lifting. A pathologic fracture was found on radiography, which on biopsy proved to be a plasmacytoma. PET-MR was obtained for further staging, revealing bilateral rib fractures (red arrows)



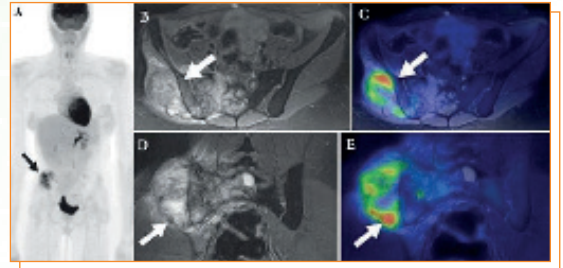
Neoplastic

Chondrosarcoma

MIP FDG images revealed regional activity corresponding to infiltrating intensely avid mass lesion related to the right iliac bone and right sacral ala having extra osseous sizable avid component infiltrating the right gluteal muscles

Note the most avid part of the lesion is that of extra osseous component [more suitable for biopsy]

pathologically proven chondrosarcoma

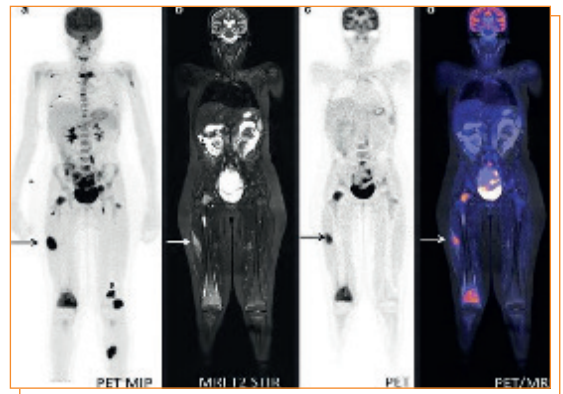


Rhabdomyosarcoma

A 13-year-old girl with neurological symptoms and pain in the right knee

a) PET MIP demonstrates widespread foci of FDG-accumulation suspected for disseminated malignancy

b-d) Coronal MRI T2 fat sat, FDG-PET, and fused PET-MR show soft tissue and BM lesions. Biopsy from the most avid lesion in the RT thigh (arrow on a-d) revealed the diagnosis metastatic rhabdomyosarcoma



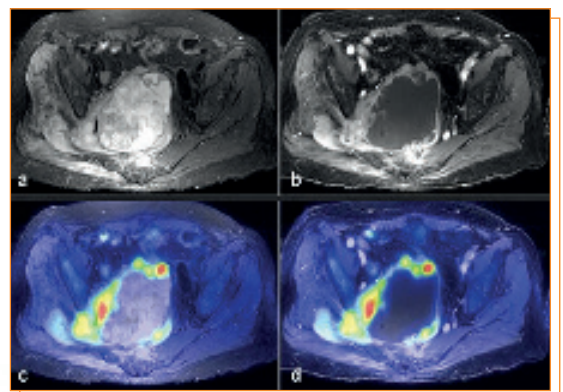
Peripheral Nerve Sheath Tumor

A 61-year-old female with a large pelvic mass discovered on CT and nondiagnostic biopsies taken during laparoscopic exploration

(a) T2-weighted fat-saturated (FS)

(b) FS post-gadolinium spoiled gradient recalled (SPGR)

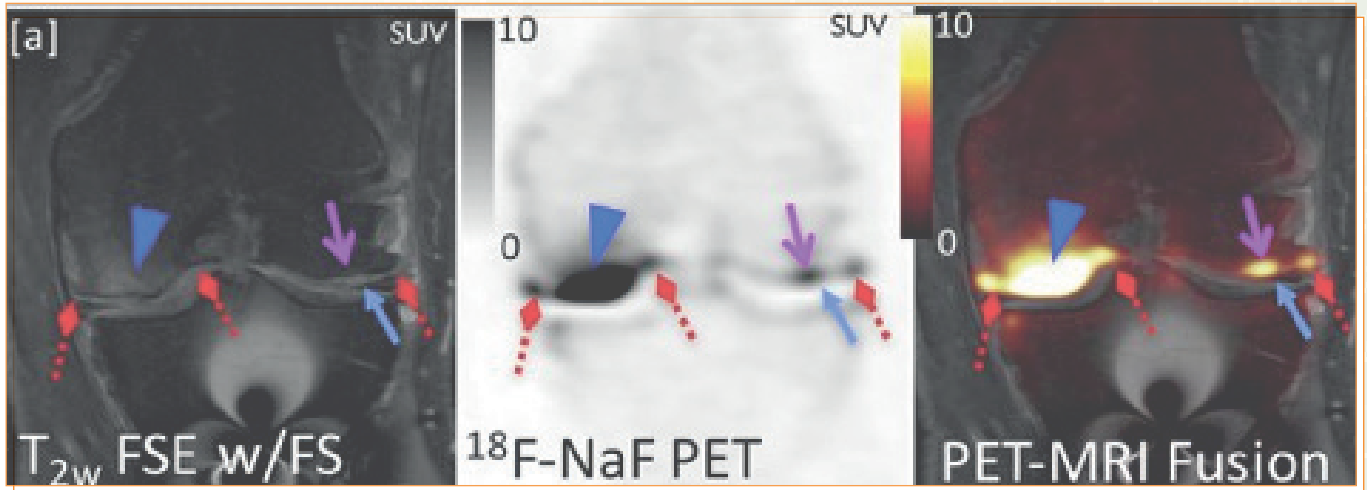
demonstrate a large heterogeneously T2-hyperintense pelvic mass extending through the right sciatic notch with peri-lesional edema and extensive central necrosis



Corresponding fused T2-weighted FS (c) FS post-gadolinium SPGR FDG PET-MRI (d) images demonstrate intense peripheral FDG activity. An FDG-avid area was targeted during subsequent CT-guided biopsy, with pathology showing a high-grade malignant peripheral nerve sheath tumor

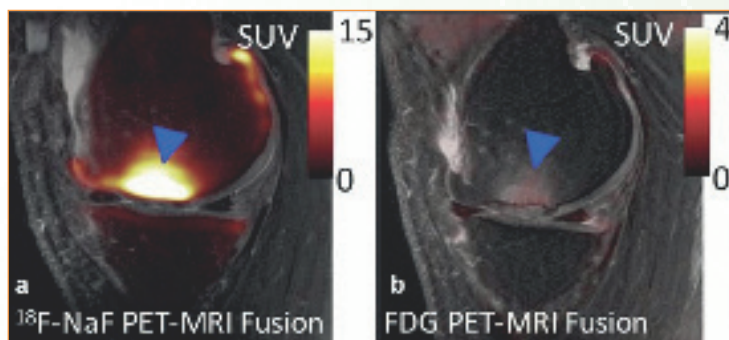
NON - NEOPLASTIC

Post-traumatic osteoarthritis



MRI, ¹⁸F-NaF PET and Fusion images of 3 patients with posttraumatic osteoarthritis (a) Concordance is seen between a BML (blue arrowhead) and large osteophytes (red diamond arrows) on MRI and high ¹⁸F-NaF uptake on PET. However, PET was able to provide additional quantitative information about metabolic activity in the knee

Osteoarthritis



¹⁸F-NaF (a) and FDG PET (b) overlaid on a T2-weighted, fat suppressed FSE MRI image acquired simultaneously in a 52-year-old male subject with OA. A large grade 3 BML (blue arrowhead) seen on MRI corresponded to considerably elevated ¹⁸F-NaF uptake (SUV_{max} 5 26.2) and only marginally elevated FDG uptake (SUV_{max} 5 1.4) relative to normal appearing bone on MRI. Imaging with multiple tracers may offer a better understanding of the etiology of features associated with OA pain and progression, such as BMLs.

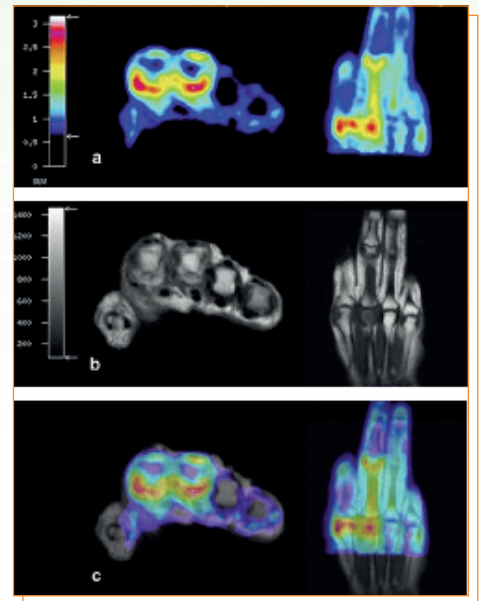
NON - NEOPLASTIC

Rheumatoid Arthritis

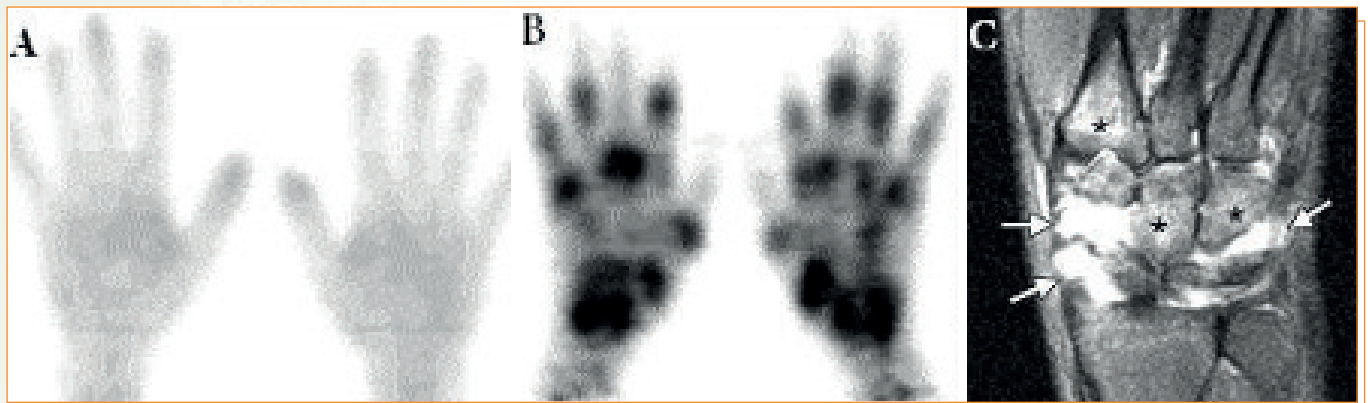
Hand in early RA acquired on an integrated PET-MRI system

- a) Axial and coronal FDG PET
- b) T1-weighted MRI
- c) overlaid fusion

The highest uptake is seen at the palmar portion of the second metacarpophalangeal joint which corresponds to synovial thickening and contrast enhancement on MR



Rheumatoid Arthritis



(A, B) 3D MIP projection image of ^{18}F -FDG uptake in a (A) healthy subject and (B) a subject with rheumatoid arthritis of the hand and wrist. ^{18}F -FDG PET can assess the metabolic activity of synovitis and has been correlated with underlying disease activity (C) MRI Coronal STIR of a subject with early rheumatoid arthritis of the wrist and normal radiographic findings. Synovitis can be observed as high signal intensity (arrows) as can bone marrow edema - asterisks

MRI provides high-resolution anatomical images to assess structural changes for diagnosis and staging of RA disease. Hybrid PET-MRI systems offer to combine high-resolution morphologic images with early molecular markers to enhance the study of RA. Also, the SUVmax of painful or swollen articulations were significantly higher than those in asymptomatic joints. Metabolic activity was significantly different between remission and active phases of arthritis

NON - NEOPLASTIC

Spondylodiscitis

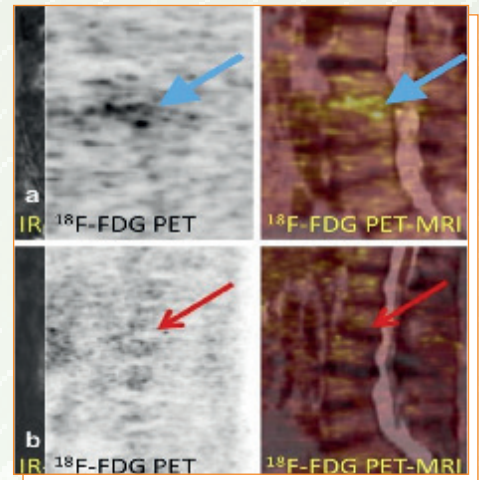
Simultaneous ^{18}F -FDG PET-MRI of patients with suspected spondylodiscitis

(a) 71-year-old

(b) 59-year-old

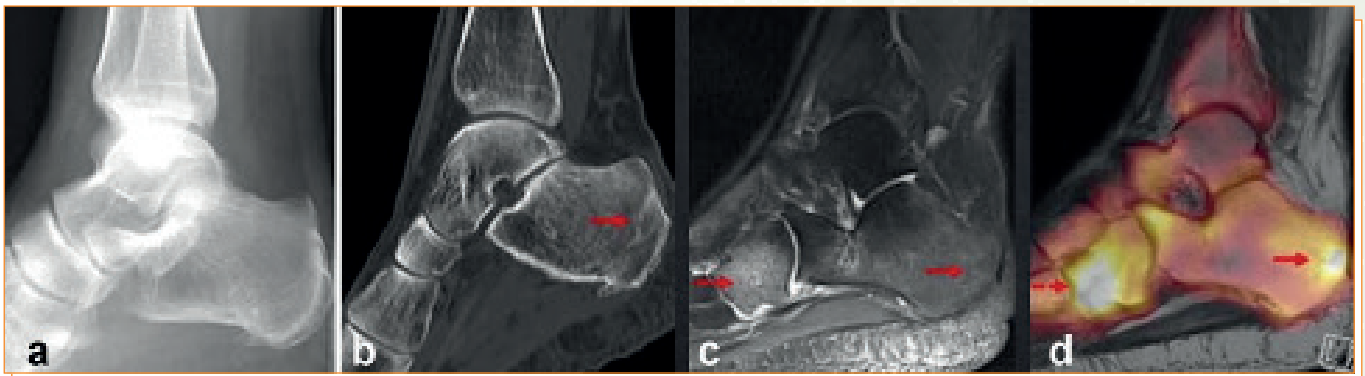
In both cases, MRI was inconclusive with typical hyperintense signal alterations on IR-FSE and moderate (a) to poor (b) postcontrast signal on T1-weighted MRI

Fused ^{18}F -FDG PET-MRI images in case



(a) showed increased uptake in the suspected discs (blue arrows) which signaled active inflammation and confirmed a diagnosis of spondylodiscitis, while the lack of elevated uptake (red arrows) in case (b) excluded active inflammation resulting in a diagnosis of no spondylodiscitis but post fracture changes

Stress Fracture



(a) X-ray

(b) CT

(c) MRI

(d) ^{18}F -NaF PET-MRI fusion of the ankle of a 58-year-old female patient X-ray images were negative, while CT show sclerotic lesions in the dorsal calcaneus (red arrow) and degenerative changes in the talonavicular region but no signs of acute stress fractures. On MRI, a fracture line in the dorsal calcaneus with little edema is seen, due to an older stress fracture that corresponds to elevated ^{18}F -NaF PET uptake - red arrow. Additionally, another stress fracture is shown on PET-MRI in the mediodorsal parts of the cuboid with bone marrow edema on MRI and elevated uptake on ^{18}F -NaF PET (dotted arrow)

مركز مصر للأشعة MISR RADIOLOGY MRC CENTER



فرد التجمع الخامس

القادم من التسعين الجنوبى أمام علامة مصر للأشعة بين المستشفى الجوى و كمبوند ليك فيو
القادم من التسعين الشمالى أمام علامة مصر للأشعة بين مستشفى شفاء و كمبوند ليك فيو

19773
01211114091

 misradiologycenter
www.misradiologycenter.com